Visualization studies of cloud-like flows

L. Venkatakrishnan*, G. S. Bhat*, A. Prabhu* and R. Narasimha*,†,§

*Centre for Atmospheric and Oceanic Sciences, Indian Institute of Science, Bangalore 560 012, India
†Fluid Dynamics Unit, Jawaharlal Nehru Centre for Advanced Scientific Research, Bangalore 560 064, India

This paper reports a series of flow visualization studies in which cloud-like off-source volumetric heating is injected into fully developed turbulent flow, with the objective of simulating the effect of the heat release that accompanies condensation and freezing of water vapour in a cloud. The visualizations provide axial and normal sections of the flow using laser sheet illumination. Special emphasis is placed on a comparison of the results obtained in jets and plumes. Although the results are broadly similar in both flows, the plume (which should be closer to a cloud) shows greater dilution due to entrainment before heating, and stronger effects due to heating. In particular, heating is shown to arrest the spread of the plume and cause considerable disruption of the large eddies in the flow. It is concluded that heat release due to phase change in a cloud has not only thermodynamic but subtle and important fluid-dynamical consequences as well.

WHEN atmospheric air ascends vertically, e.g. in the form of a plume from a hot spot on the ground, there is a drop in its temperature due to adiabatic expansion. When there is sufficient moisture present (as is usually the case in the tropics), the ascending air becomes saturated with respect to water vapour at some level. Further ascent leads to condensation of excess water vapour into liquid drops or ice particles. This mixture of dry air, water vapour and condensed or frozen water is what constitutes a cloud (see refs 1, 2 for a detailed analysis of cloud microphysics). From the dynamical point of view, phase change has many consequences. A series of experiments being carried out at the Centre for Atmospheric and Oceanic Sciences, Indian Institute of Science[3,4] suggests that the most important fluid-dynamical consequence may be the warming of the cloud by the release of latent heat. Each gram of water vapour condensing to liquid releases about 2.5 kJ of heat, which is sufficient to warm 1 kg of cloud air by 2.5°C. (The figures for freezing are 0.33 kJ and 0.3°C.) For air at constant pressure, small changes in temperature T and density ρ are related to each other (using the perfect gas law) according to the equation

$$\frac{\Delta T}{T} = -\frac{\Delta \rho}{\rho}. \qquad (1)$$

§For correspondence. (e-mail: roddam@caos.iisc.ernet.in)

Hence the warming results in an increase in buoyancy, thus aiding further ascent of the cloud mass and overcoming the adiabatic cooling of the rising air, resulting in a temperature difference of some 0.5–1°C above the surroundings. More specifically, because of the relatively large value of the latent heat of condensation of water vapour, atmospheric conditions can be conditionally unstable, i.e. the thermodynamics of adiabatic processes in humid air is such that, over a range of ambient temperature lapse rates, a parcel of air can rise if it is saturated but descend if it is dry (see e.g. ref. 2, p. 31). Under conditions favourable to the growth of a cloud, therefore, a parcel of saturated air can be slightly warmer than the ambient and keep ascending, and also simultaneously be cooler than the condensation temperature and keep condensing. An estimate of the (negative) Richardson number, which provides a measure of the ratio of buoyancy to inertial forces, suggests values in the range 0.2–0.4, indicating that the enhanced buoyancy due to released latent heat can be significant[3].

Of course condensation (and freezing, when that also takes place) will render cloudy air a multi-phase fluid. Even otherwise, a cloud is a complex phenomenon in which microphysics and thermodynamics play important roles. But while these roles have been extensively studied[1,2], far less attention has been paid to the fluid-dynamical aspects of the problem, which present some intriguing puzzles (as we shall discuss shortly). The objective of the present study is to look at one aspect of the fluid dynamics of the cloud, namely the effect of heat release due to phase change, through a laboratory simulation of cloud-*like* off-source heating in two relevant turbulent flows.

If the details of the phase change are put aside for a moment, then flow inside a cloud is characterized by a local increase in temperature and hence buoyancy. While vertical ascent is required for cooling and condensation, the heating rate produced depends on the amount of water vapour that is condensing or freezing. It must be realized that a jet (for example), subjected to such heating, does not merely become the standard (and much-studied) hot jet, i.e. jet of pre-heated fluid, in which the temperature and velocity distributions are inter-related and the relevant scales of both variables evolve together. When the temperature varies independently of the velocity, as may happen, e.g. by

combustion or by volumetric heating of the fluid *away from the source of the flow*, the velocity and temperature scales cease to be inter-related as in a hot jet. The mechanism governing the flow behaviour under such conditions is poorly understood. It is this class of flows with off-source generation of buoyancy – of which cumulus clouds are a naturally occurring example – that we seek to understand in the present series of studies.

One parameter of great interest in these flows (and in clouds) is entrainment. Most early cloud models assumed entrainment of ambient air into the cloud from its lateral edges, and employed an entrainment relationship of the type conceived first by Taylor[5], which postulates that the mean inflow velocity across the edge (say V_e) of a free turbulent shear flow is proportional to a characteristic velocity within the flow, usually taken as the local time-averaged maximum mean velocity at the level of inflow (U_c). Taylor's hypothesis has been successful in a variety of situations, but when applied to clouds it has failed to make realistic predictions of either liquid water concentrations or height of penetration[6,7]. Studies such as those by Paluch[8] showed that the observed thermodynamic properties in a cloud could be accounted for only if air from the cloud base rose to the top *without* lateral mixing with the surrounding air. In fact the composition of cloud air near the cloud top shows that it results from mixing of the ambient air near the cloud top with that from the cloud base (this is the phenomenon of so-called cloud-top entrainment); only in regions much below the cloud top is there evidence for lateral mixing[9]. Such lack of entrainment was also suggested for cumulonimbus clouds over the tropics by Riehl[10]. Thus Taylor's entrainment hypothesis does not appear to be valid for such flows. Emanuel[11] points out that early cloud parameterization schemes, based on such a hypothesis and leading to what has been called the similarity entraining plume model, were later thoroughly discredited by observations. (An ideal plume is a flow driven by a source of buoyancy like an area of high temperature over a solid surface, with no momentum flux at its origin; in contrast, a jet is driven by the efflux of momentum through a nozzle. A jet of hot fluid issuing into cold surroundings can, however, transform itself into a plume over a distance of a few so-called Morton length scales, to be defined below.) If such a (one-dimensional) plume model is tuned to match the observed liquid water content, the model air is too cold to ascend to the observed cloud heights; if tuned to match the observed cloud tops, the liquid water content is over-predicted[7]. Also the velocity and length scales are negatively correlated for laterally entraining plumes and thermals[12], whereas there is no evidence to support such a tendency in cumulus or cumulonimbus clouds[13]. Therefore the flow inside clouds is very different from that in classical jets and plumes, where the ambient air is continuously drawn into the flow and mixed thoroughly.

An earlier effort that investigated fluid-dynamical issues of this kind is the work of Elavarasan *et al.*[3], who reported extensive exploratory studies of volumetrically heated jets. It was found that, with a sudden increase in buoyancy, there was indeed a marked change in flow behaviour compared to that in a neutrally buoyant jet. Bhat and Narasimha[4] have presented a detailed analysis of the data from these and other experiments. It has however been felt that a jet, being a momentum-driven flow, may not be a close enough analogy for a cloud, which is modelled better by a plume[12]. Plumes, like jets, have been studied extensively, and a reasonably good understanding of their behaviour exists[12,14–16]. Hence the characteristics of the plume generated for this study in the absence of off-source buoyancy enhancement can be validated against data available in the literature.

We consider here an idealized cloud arising from an axisymmetric plume as shown in Figure 1. The plume is generated due to a hot spot on the terrestrial surface; once this plume starting from the hot spot crosses the lifting condensation level (at which the air becomes saturated with respect to water vapour), it is visible as a cloud, but this visible cloud is only the crown of an invisible plume stretching all the way to the ground. In the experiments described here, on the other hand, the *whole* plume is visualized, i.e. both below and beyond the level where heat injection (corresponding to the level of condensation in the natural cloud) starts.

In this paper we report a *comparative* study of jets and plumes. There is one important reason for undertaking such a study. With off-source addition of heat

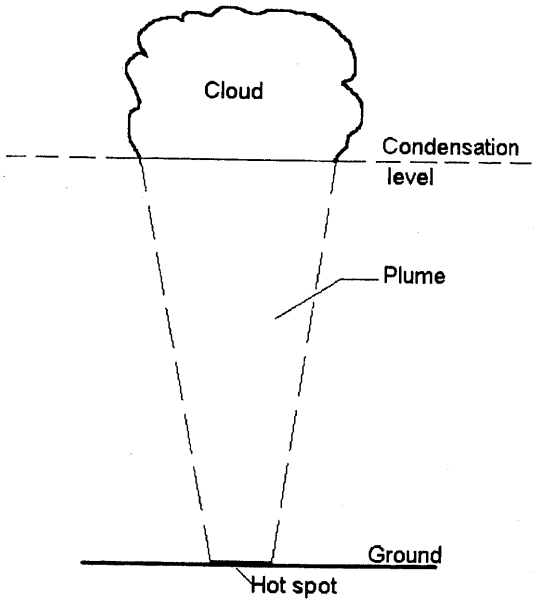

Figure 1. Idealized cloud arising from an axisymmetric plume.

in a jet, the question that naturally arises is whether the changes one observes are to be attributed to a possible transition from the momentum-dominated jet (before heating) to the buoyancy-dominated plume (after heating). If this were true, the structure of the jet after injection of (off-source) heat should resemble that of a plume. A direct comparison can settle whether this proposition is valid. Here we report such a comparison.

In order to assess the differences between a jet and a plume in terms of differences in eddy structure, especially following buoyancy enhancement, some of the experiments of Elavarasan *et al.*[3] have been repeated for a carefully selected set of flow parameters using the current set-up. We present here a comparison of instantaneous flow visualization pictures to achieve the above objective.

The appropriate non-dimensional parameter governing the effect of heat release, as proposed by Bhat and Narasimha[4], relates the volumetric heat input with the energy flux with which the flow enters the heat injection zone in the plume, and is given by

$$G = \frac{\alpha g}{\rho C} \frac{Q}{b_b U_b^3}, \tag{2}$$

where Q is the total volumetric heat input, b_b and U_b are the velocity half-width and centreline velocity respectively at the beginning of the heat injection zone, C is the specific heat, α is the coefficient of cubic expansion of the fluid and g is the acceleration due to gravity. In most of the experiments reported here, this number has been set to the value $G = 0.25$, which is typical of conditions in cumulus clouds as Table 1 shows. The experiments therefore achieve fluid-dynamical similarity with the idealized cloud-plume as far as buoyancy effects are concerned; Reynolds numbers are of course much lower in the experiments than in the atmosphere, but jets and plumes are known to become relatively insensitive to Reynolds number at modest values of the parameter, in particular because these flows are highly unstable (with critical Reynolds numbers of order only 1 to 10).

Experimental set-up

A schematic of the flow configuration and the experimental arrangement is shown in Figure 2. The arrangement for the jet has been described by Elavarasan *et al.*[3]. The vertical axisymmetric plume is generated in the same water tank, of dimensions 600 mm × 600 mm × 1200 mm. The diameter of the nozzle from which the plume issues is $d = 4$ mm. The enhancement of buoyancy is achieved by the volumetric heat injection method developed by Bhat *et al.*[17], based on direct ohmic heating of a conducting liquid. The heating is achieved by application of a 20 kHz alternating voltage across electrodes, each of which is a grid of fine platinum wires. Heat is added over the region from $50\,d$ to $83\,d$ from the source.

The tank is filled with filtered and de-ionized water to ensure a non-conducting ambient fluid. The plume is generated by means of an electric heater enclosed in a perspex heating chamber. The active fluid (de-ionized water made electrically conducting by means of addition of hydrochloric acid) is supplied to the plume heating chamber by means of a variable height constant level tank. The temperature difference between the plume and the ambient at nozzle exit is maintained at 55°C by appropriate variation of the voltage supplied to the heater and the height of the constant level supply tank. The Morton length scale for the flow, defined as

$$l_M = \left(\frac{\pi}{4}\right)^{\frac{1}{4}} \left(\frac{\rho_a d U_{exit}^2}{g\,|\Delta\rho|}\right)^{\frac{1}{2}} \tag{3}$$

(where ρ_a is the ambient density, $\Delta\rho$ is the difference between the ambient and local mean density and U_{exit} is the velocity at the nozzle exit), is about 16 mm or $4d$. From the work of Papanicolau and List[16], we may expect a fully developed plume beyond $z = 5\,l_M$, i.e. about $20d$ in the present case.

The structural differences in the flow are examined by visualizing the flow using the laser-induced fluorescence technique, with Rhodamine 6G as dye and a

Table 1. Estimation of G for clouds and for the present flows

Flow	Width b (m)	Centre-line velocity U_c (m/s)	$\Delta\rho/\rho \times 10^3$	G
Cumulus (Ludlam[26])	500	3–4	0.2–1.7	0.11–0.53
Cumulonimbus (Ludlam[26])	1200–2500	10–25	3.5	0.14–0.46
Jet/plume $d = 4$ mm, $z/d = 50$ $Q = 555$ W	21×10^{-3}	38×10^{-3}	1.58	0.25

300 μm thick laser sheet from a 4 W argon ion laser. Still photographs were taken utilizing a Canon EOS 1000 still camera, and a video recording with a National (model NV-M5EN) VHS video camera (at a recording speed of 25 frames per second). A detailed description of the instrumentation for the flow visualization technique can be found in Bhat and Narasimha[4] and Bhat[18]. We present here an analysis of the still photographs.

Laser-sheet imagery

The results for the flow visualization of the jet are shown here at a fixed Reynolds number and heating rate. The Reynolds number is 2005, based on the nozzle diameter and an exit velocity of 0.47 m/s. In the range of Reynolds numbers covered by Elavarasan *et al.*[3], it was seen that at Re = 1600 there were small deviations from the self-preserving behaviour due to low-Reynolds number effects, and at Re = 3200 the effect of heating was not appreciable due to the high flow velocities in the heat injection zone. Based on this experience, a Reynolds number of around 2000 has been selected as an optimum value for the present jet experiments. In the plume the exit velocity is 0.16 m/s, giving a plume Reynolds number of 670. This value was selected for the experiment by the criterion that the specific momentum flux of both jet and plume flows be of the same order when they enter the heating zone, so that the structures causing entrainment could be compared under similar conditions. Turner[15] has pointed out that the specific momentum flux may play an important role in entrainment dynamics. Because of the difference between jet and plume in decay and entrainment rates, the flow conditions selected provide the same momentum flux at entry to the heat injection zone in both plume and jet. It should be recalled here that, in a jet with an end wall in the proximity of the nozzle (as in the present experiments), the momentum flux does not remain constant but tends to *decrease* as we move downstream (see Schneider[19]), whereas for a plume the momentum flux tends to *increase* due to the constant buoyancy flux. This was checked to be true in the present experiments by integration of LDV-measured velocity profiles.

In the following sections, the observations from the flow visualizations are presented.

Vertical cross-sections

Figure 3 *a* shows instantaneous vertical sections of the unheated and heated jet from the experiments reported in Bhat and Narasimha[4], at a volumetric heat injection rate of Q = 700 W which corresponds to $G = 1.6$ – considerably higher than the value chosen here for the plume ($G = 0.25$), for reasons which will become apparent in the following section. The thin dark lines in the horizontal direction are the shadows of the wire frames (situated *outside* the flow) that support the electrode wire grids across which heating is applied. It is seen that the grids have no noticeable effect on the structure of the flow. The brighter regions contain the jet fluid, while the darker regions correspond to the ambient. Some dark

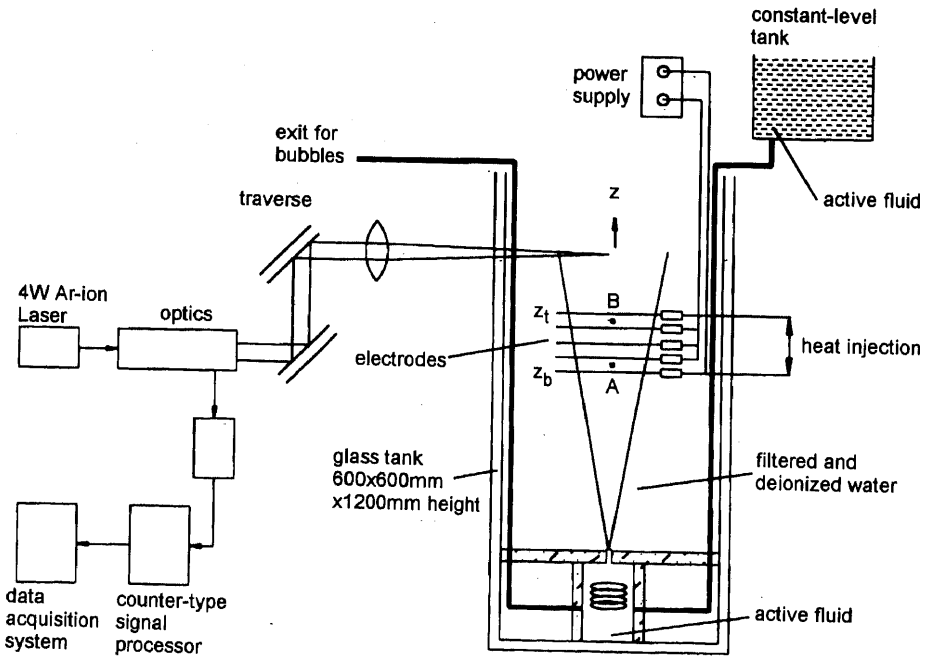

Figure 2. Schematic of experimental arrangement.

patches are seen even in the vicinity of the jet axis, implying the presence of essentially unmixed ambient fluid there. This ambient fluid is engulfed into the main flow by large coherent vortices present in the jet. Previous investigations, by Brown and Roshko[20] on free shear layers and later by Dahm and Dimotakis[21] and Papantoniou and List[22] in jets, have shown that the existence of large scale organization of the flow in the form of vortical structures with significant coherence is a characteristic feature of turbulent shear flows. These structures, clearly seen in the figure and consistent with those reported by Dahm and Dimotakis[21], bring in the ambient fluid and are thus basically responsible for turbulent entrainment. Detailed correlation measurements using hot wires by Tso and Hussain[23] also show the presence of structures of several types in a jet, including toroidal and helical vortices.

It can be clearly seen from Figure 3 *a* that the width of the jet increases almost linearly with downstream distance, and the large scale structures grow proportionately in size. These observations are in agreement with previous work. It is further seen that the structure of the preheating zone in the heated case (Figure 3 *b*) is similar in nature to that in the unheated case. In zone II (the heat injection zone, see Figure 2), however, the eddies are not as sharply defined, and the horizontal extent of the eddies has diminished and lateral growth is inhibited. The region near the jet axis also shows greater uniformity in dye concentration, consistent with lower engulfment and hence less dilution. It has been proposed[4] that the changes seen are an indication of disruption of the eddy structure in the heat injection zone, and that such disruption is responsible for lower entrainment. It is also seen from the figure that immediately after the heat injection zone, instabilities begin to reappear in the outer region of the jet and gradually extend to the axis. This behaviour is similar to that observed in the zone of flow establishment where instability of the shear layer leads to the generation and growth of large scale vortical structures as reported by Hirst[24] and Liepmann and Gharib[25]. The extent of this zone of flow establishment in the post-heating zone is seen to be about two to three times the jet width at the top of the heat injection zone.

Figure 4 *a, b* shows instantaneous vertical sections respectively of the unheated plume and the heated plume at $Q = 555$ W ($G = 0.25$). It is seen that (Figure 4 *a*), as in the jet, the width of the plume increases almost linearly with downstream distance in the absence of heat injection, and that the large scale structures grow proportionately in size, as expected. With heat injection (Figure 4 *b*), the flow in and up to the end of zone I (indicated by the first dark horizontal line) remains unaffected; however on the introduction of volumetric heat the large eddies are disrupted and the linear growth of the plume is arrested. No ambient fluid is any longer seen in the central region of the plume.

Figure 5, which shows a close-up view of the unheated plume, highlights the visual differences seen between

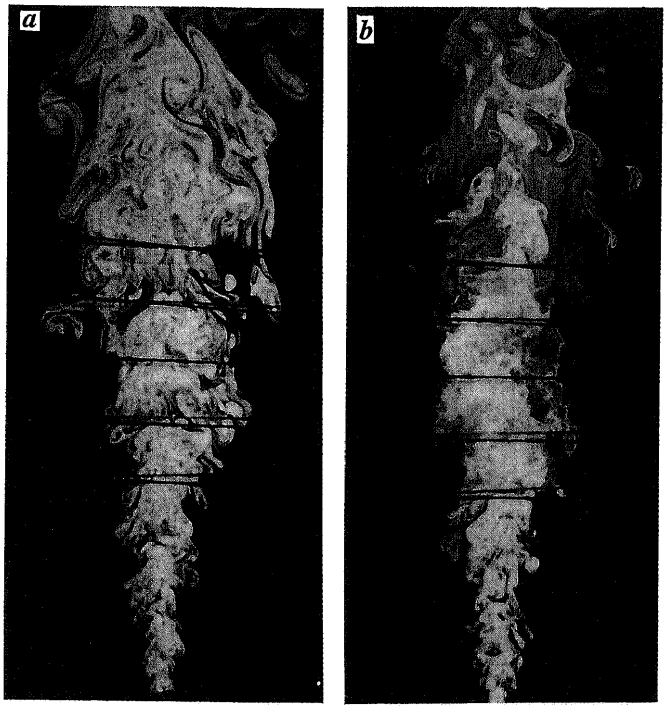

Figure 3. Vertical cross-sections of the (*a*) unheated and (*b*) heated jet at $G = 1.6$.

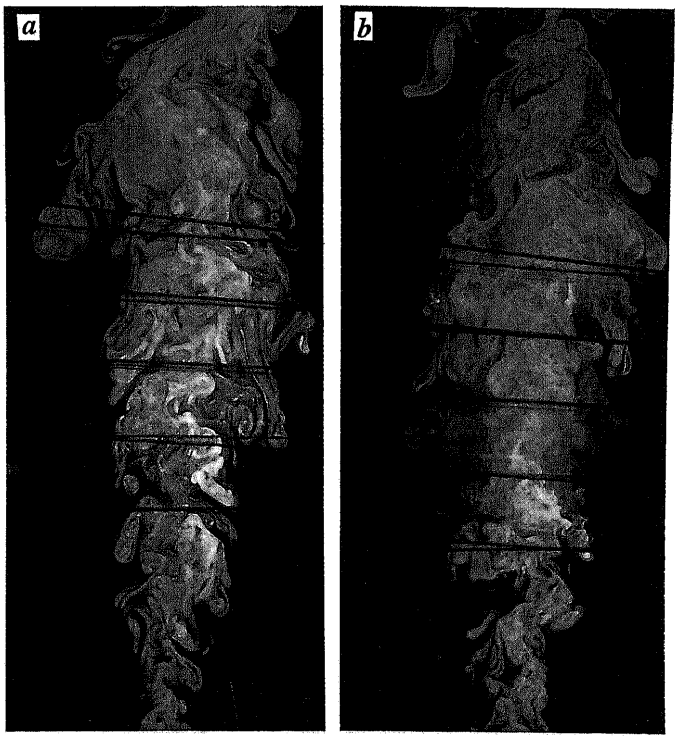

Figure 4. Vertical cross-sections of the (*a*) unheated and (*b*) heated plume at $G = 0.25$.

the plume and the jet. It can be seen right away that the structures in the unheated plume seem to be more 'complex' compared to those in the unheated jet of Figure 3 *a*. The eddies seen near the edges of the plume seem to be coiled, spring-like structures. The structures seen in the vertical cross-sections of the jet appear to be much less elongated in shape.

Figure 6 shows a plume with volumetric heating. The flow up to the beginning of the heat injection zone is unaffected and shows an interesting feature in the more highly intermittent flow in the plume compared to a jet: although the flow at the exit is steady, there is a striking 'hole' in the picture, showing that one can move in a continous line all across the flow without encountering any plume fluid! (We should remind ourselves that the picture is a two-dimensional section, so what we are observing is most likely a hole through the plume and not necessarily a complete rupture of the plume into two disjoint parts.) An examination of the lower part of the figure also shows (like Figure 5) that, compared to the unheated jet (Figure 3 *a*), much more entrained ambient fluid is carried across to the centreline of the plume, i.e. ambient fluid appears to penetrate deeper into the flow. An examination of the videos showed this to occur more often in a plume than in a jet, demonstrating the greater entraining power of the former.

Figure 7 *a*, *b* shows vertical cross-sections of the unheated and heated plume, both averaged over 40 frames. (This averaging is carried out over digitized images of the flow from the video; a false-colour image is then obtained by assigning colour values to each pixel in the image depending on the dye concentration in the pixel, as shown by the colour bar in the figure.) The shrinking of the yellow region shows clearly the suppression of plume growth on heat addition: the nearly uniform dye concentration in the central region of the heated plume (shown by the deep blue core in Figure 7 *b*), indicates the absence of the dilution that takes place in the unheated plume because of entrainment, and the consequent well-mixed nature of the core. Paradoxical as it may sound, the *lower* engulfment with heat addition goes with a *more* well-mixed state in the core, precisely because there is less dilution; this observation shows that one has to be extremely careful about repeating the kind of common pronouncement that identifies 'entrainment' and 'mixing'.

Pictures of the mean flow in the jet have already been presented by Bhat *et al.*[17], and so will not be repeated here. In general the effect in both jet and plume flows is similar, but the absence of diluting entrainment is more dramatic in Figure 7.

Horizontal cross-sections

Figure 8 *a–c* shows horizontal cross-sections of the jet at a height above nozzle exit of 317.5 mm ($z/d = 79.4$, just before the completion of heat addition) with volumetric heat injection rates of $Q = 0$ W ($G = 0$), $Q = 700$ W ($G = 1.6$, from the experiments of Bhat and Narasimha) and $Q = 555$ W ($G = 0.25$) respectively. Figure 8 *d* shows the section at 30 mm beyond the heat injection zone ($z/d = 86.9$). (It should be noted that the differing intensities in these pictures have no significance and reflect natural variations in experimental procedure as they were taken during different experimental runs and sometimes with a green colour filter instead of a yellow filter.)

Figure 8 *a* indicates that the instantaneous structure of the jet is far from being axisymmetric and a number of eddies extend into the ambient fluid. These tongue-like eddies engulf the ambient fluid and bring them into the main flow. In Figure 8 *b*, the structure of the jet is not as clear as in the unheated jet; some eddies can be seen at the edges but they do not extend as far out radially as in the case of the unheated jet. Furthermore, the edges appear diffuse and the boundaries less sharp. The changes are indeed striking when compared with the unheated case (Figure 8 *a*); the large structures appear to have completely vanished and the jet has shrunk appreciably with heat injection. There is hardly a trace of the ambient fluid inside the jet. From Figure 8 *c*, which shows the jet at $G = 0.25$ (the same value as for the plume), it is seen that the degree of disorganization is far less than seen in the jet at $G = 1.6$ – a point we shall return to later after examining the plume at the corresponding height and G. Beyond the heat injection zone (Figure 8 *d*) an incipient re-emergence of eddy structure is seen and the jet boundary seems sharper.

It is interesting to compare the above features with Figure 9 *a*, *b*, which shows diametral sections of the plume without and with heat injection ($Q = 555$ W, $G = 0.25$) respectively. The sections are taken at the same height as for the jet ($z/d = 79.4$). From Figure 9 *a* it is seen that here too, as in the jet, the plume is far from being instantaneously axisymmetric and a number of eddies extend into the ambient fluid, engulfing it into the main flow. However the number and distribution of these eddies are very different (cf. Figure 8 *a*), suggesting that the plume has a much richer structure than a jet.

Figure 9 *b* shows the horizontal cross-section of the heated plume at the same location as Figure 9 *a*. The edges are no longer sharply defined, and there is a more nearly homogeneous structure with well-mixed dye (plume fluid) in the core near the axis. The tongues of plume fluid no longer extend into the ambient as in Figure 9 *a*, and little ambient fluid is seen in the core of the plume. All these features are consistent with those seen in the vertical sections of Figure 7.

It is illuminating to compare the plume section seen in Figure 9 *b* with the horizontal cross-section of the

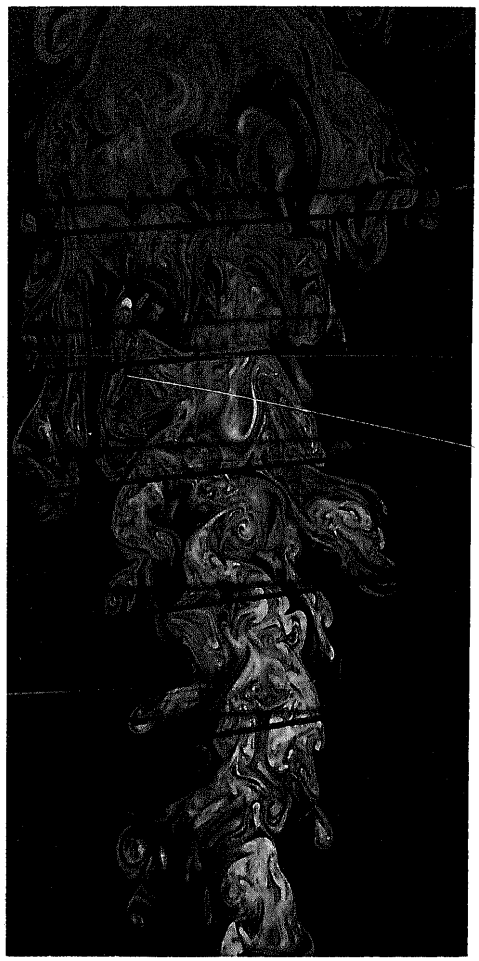

Figure 5. Close-up view of the unheated plume showing the detail of the eddy structure.

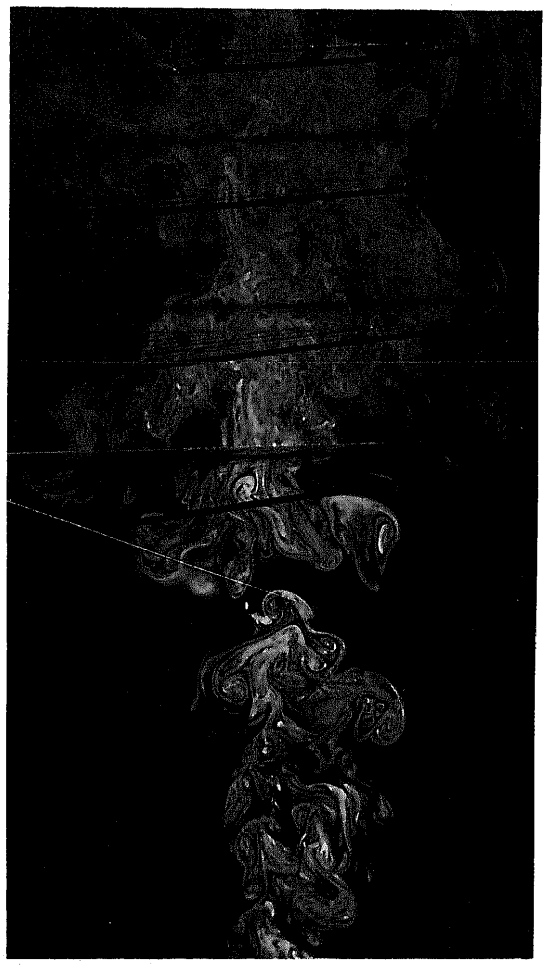

Figure 6. Close-up view of the heated plume showing the intermittent nature of the flow.

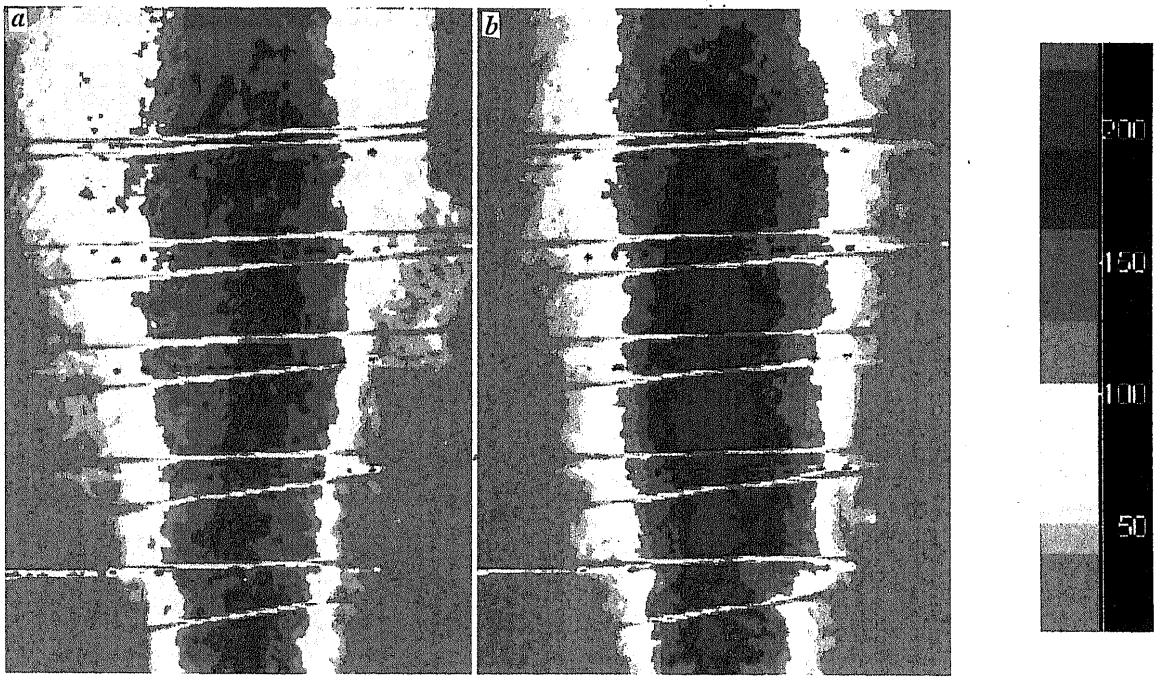

Figure 7. Average pictures of vertical cross-sections of the (*a*) unheated and (*b*) heated plume.

jet at the same location with $Q = 700$ W, shown in Figure 8 *b*. Revisiting Figures 5 *b*, *c* and 6 *b*, it is seen that the disorganization achieved already at $G = 0.25$ in the plume is similar to that reached only at $G = 1.6$ in the jet. The jet at $G = 0.25$, as pointed out earlier, still shows traces of ambient fluid at the centre, and its edges do not appear as diffuse as those of the plume at $G = 0.25$.

These visualizations of the flow demonstrate that, at nearly the same Reynolds numbers, a far higher level of disorganization is achieved in the plume at a much lower heating than is required in a jet. Thus, the effect on entrainment due to heat release may be expected to be even stronger in a plume than what has been earlier observed in a jet.

Finally, comparing the flow in the jet *after* heat addition (i.e. in the post-heating zone) (Figure 8 *d*) with that in a plume *before* heat addition (Figure 9 *a*), we can see that the effect of volumetric heat addition of the kind implemented here cannot be looked upon as just a transition from jet to plume. For the parameters governing the present experiment, the structural changes observed are far stronger than would be consistent with such a transition, which (if occurring at all) must be presumed to lie much farther downstream than the region covered in the experiment.

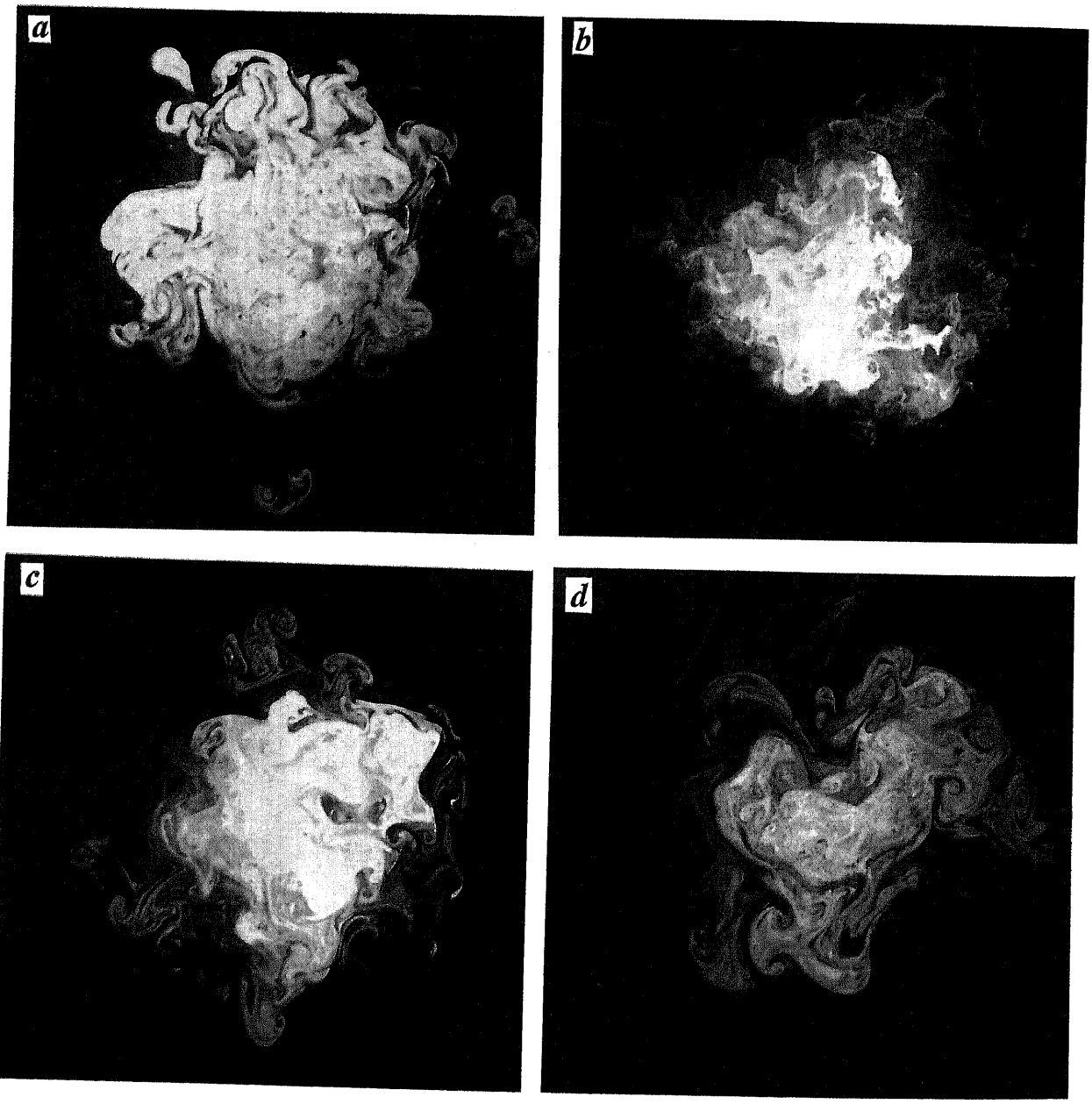

Figure 8. Diametral sections of the jet (*a*) $G = 0$, (*b*) $G = 1.6$, (*c*) $G = 0.25$ at $z/d = 79.4$; (*d*) 30 mm beyond heat injection zone, $z/d = 86.9$.

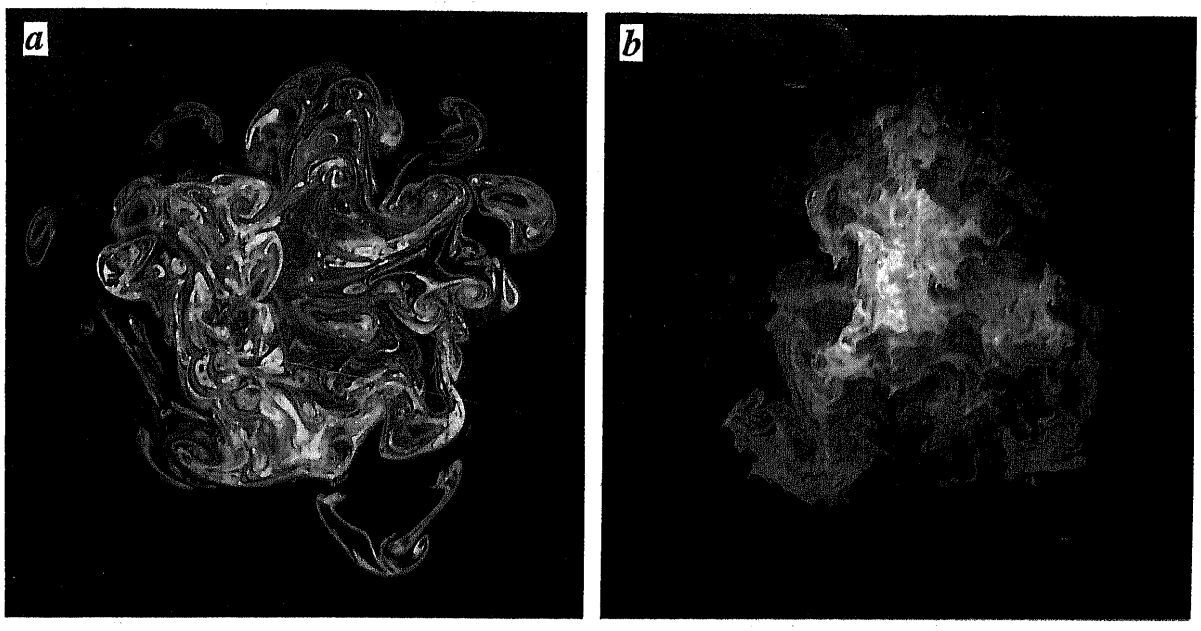

Figure 9. Diametral sections of the (*a*) unheated and (*b*) heated plume at $z/d = 79.4$.

Conclusions

The studies reported here lead to the following conclusions.

The horizontal cross-sections at different streamwise locations show that the eddy structure of the flow is qualitatively similar in both jets and plumes, but the number and distribution of such structures is very different, suggesting that the plume has a richer structure.

The structure and dynamics of an axisymmetric plume are considerably altered when the buoyancy is enhanced locally by volumetric heating. This change is similar to that seen in the jet but is much stronger, i.e. comparable changes occur at much lower values of heat injection. The volumetric heating is seen to arrest the spread of the plume and causes considerable disruption of the large eddies in the flow.

From a comparison of the horizontal cross-section of the *heated* jet after zone II with that of the *unheated* plume at the same location, it is found that the re-emerging eddy structures in the heated jet differ from those in the plume, suggesting that what is observed in the heated jet is not a mere transition to a plume.

The large vortical structures present in the unheated jet or plume (thought to be responsible for engulfment of ambient fluid into the flow) having been disrupted by the heating, the flow appears diffuse in the heat injection zone. Again, from the present flow visualization studies, the disruption for the same value of heating appears to be far greater for plumes than for jets.

It is clear from the above conclusions that the volumetric heating is doing more than merely enhance the buoyancy for the jet or the plume. If the entrainment process were to be divided into three stages, namely (i) engulfment – during which the ambient fluid is inducted into the flow, (ii) mingling – when the engulfed fluid is stirred into the active fluid, and (iii) mixing – where the mingled fluid mixes at the diffusion scales by molecular interaction, the volumetric heating can be said to be arresting the first stage, namely engulfment; once this has happened, it is the fluid that was engulfed upstream (i.e. before heat injection) that is stirred and mixed, and in the absence of dilution from the ambient fluid the heated flow appears more nearly uniformly 'mixed' than the unheated flow. This is borne out by visualizations of both horizontal and vertical sections of the plume.

From the striking effects observed in the plume experiments here, it is clear that the flow in clouds (and the entrainment thereto) will be strongly influenced by the heat release that occurs on condensation and freezing: thus, such heat release has not only thermodynamic but important fluid-dynamical consequences as well.

1. Mason, B. J., *Physics of Clouds*, Clarendon Press, Oxford, 1971.
2. Rogers, R. R., *Short Course in Cloud Physics*, Pergamon, New York, 1989.
3. Elavarasan, R., Bhat, G. S., Prabhu, A. and Narasimha, R., *Fluid Dyn. Res.*, 1995, **16**, 189–202.
4. Bhat, G. S. and Narasimha, R., *J. Fluid Mech.*, 1996, **325**, 303–330.
5. Morton, B. R., Taylor, G. I. and Turner, J. S., *Proc. R. Soc. London*, 1956, **A234**, 1–23.
6. Squires, P. and Turner, J. S., *Tellus*, 1962, **14**, 422–434.
7. Warner, J., *J. Atmos. Sci.*, 1970, **27**, 1035–1040.
8. Paluch, I. R., *J. Atmos. Sci.*, 1979, **36**, 2467–2478.
9. LaMontagne, R. G. and Telford, J. W., *J. Atmos. Sci.*, 1983, **40**, 2148–2156.
10. Riehl, H., *Climate and Weather in the Tropics*, Academic Press, New York, 1979.

11. Emanuel, K. A., *Atmospheric Convection*, Oxford University Press, Oxford, 1994, p. 540.
12. Turner, J. S., *Buoyancy Effects in Fluids*, Cambridge University Press, 1973.
13. LeMone, M. A. and Zipser, E., *J. Atmos. Sci.*, 1980, **37**, 2444–2457.
14. Rouse, H., Yih, C. and Humphrey, S. H. W., *Tellus*, 1952, **4**, 201–210.
15. Turner, J. S., *J. Fluid Mech.*, 1986, **173**, 431–471.
16. Papanicolaou, P. N. and List, E. J., *J. Fluid Mech.*, 1988, **195**, 341–391.
17. Bhat, G. S., Narasimha, R. and Arakeri, V. H., *Expt. Fluids*, 1989, **7**, 99–102.
18. Bhat, G. S., *J. Indian Inst. Sci.*, 1996, **76**, 639–649.
19. Schneider, W., *J. Fluid Mech.*, 1985, **154**, 91–110.
20. Brown, G. L. and Roshko, A., *J. Fluid Mech.*, 1974, **64**, 775–816.
21. Dahm, W. J. A. and Dimotakis, P. E., *J. Fluid Mech.*, 1990, **217**, 299–330.
22. Papantoniou, D. and List, E. J., *J. Fluid Mech.*, 1989, **209**, 151–190.
23. Tso, J. and Hussain, F., *J. Fluid Mech.*, 1989, **203**, 425–448.
24. Hirst, E., *Water Res. Res.*, 1972, **8**, 1234–1246.
25. Liepmann, D. and Gharib, M., *J. Fluid Mech.*, 1992, **245**, 643–668.
26. Ludlam, F. H., *Clouds and Storms*, Pennsylvania State University Press, University Park, PA, 1980.

ACKNOWLEDGEMENTS. The work reported here has been supported by a grant from the Department of Science and Technology, Government of India.

Received 7 November 1997; revised accepted 29 January 1998

Possible impact of tidal frequencies on the predictability of the earth's axial rotation

R. K. Tiwari* and K. N. N. Rao

Theoretical Geophysics Group, National Geophysical Research Institute, Hyderabad 500 007, India

Short-term fluctuations in earth axial rotation, which is proxy for fluctuations in length of day (LOD), represent composite response of terrestrial coupling of ocean and atmospheric dynamics and extra-terrestrial torque (sun–moon system) of tidal reverberations. We examine here the possible influence of tidal frequencies (periodic signal) on the predictability of LOD changes using the techniques from the recent development in nonlinear dynamical system theory. The second-order Kolmogorov entropy (K_2) measures the rate of loss of information in dissipative dynamical system and defines a lower bound of the entropy. We present here a comparative study of Kolmogorov entropy (K_2) of original and filtered (tidal) LOD time series data. Our analyses indicate a contrasting sensitivity in K_2 values which correspond to predictive time limit of about 6–8 and 12–13 days for original and tidally removed (filtered) LOD data respectively. This difference of about 40–50% in coherent K_2 structures (predictive time limit) of filtered and original LOD data possibly indicates that presence of tidal signal in LOD time series enhances the degree of chaoticity and thereby limits the predictive time. It may be suggested that nonlinear resonances created by the earth's seasonal cycle and various other frequencies taking place due to thermodynamical property of the atmosphere–ocean system possibly turned the underlying dynamics to chaotic route. The understanding of these physical interactions may create physical premises for theoretical modelling of coupled ocean–atmospheric LOD dynamics and thereby allowing causally related prediction of underlying dynamics.

THE planet earth continuously changes its orientation in space under the influence of internally generated torque at the core–mantle boundary and also due to the gravitational attraction of earth–moon system. The angular rotational speed of the earth (earth's axial rotation), therefore, fluctuates and is reflected in fluctuations in length of day (LOD). Fluctuations in LOD are, therefore, proxy for earth axial rotation. The LOD signal exhibits minute but complicated changes corresponding to variations of several milli-seconds in LOD (Figure 1). These changes are caused due to the effect of a wide variety of geophysical (e.g. oceanic–atmospheric) phenomena and astronomical disturbances. Fluctuations in LOD, therefore, exhibit a composite response of coupled earth–ocean–atmosphere and astronomical system (e.g. deterministic tidal signals, stochastic weather pattern and quasi-periodic seasonal terms, etc.). Recent nonlinear analyses of LOD time series have indicated possible evidence of low dimensional strange attractors (chaos)[1,2]. The other fundamental properties of chaos include high sensitivity to the initial conditions which lead to exponential growth of disturbances in attractor regions, finite and non-zero (K_2) entropy, broad-band spectral characteristics, complex phase-space trajectories, etc.[3].

Prediction of a physical phenomenon is an interesting curiosity and ultimate goal of science. An appropriate analysis of various properties of chaotic attractor renders a way of precise forecast of the state of the dynamical system. In order to make a precise statement or quantify predictive time limit it is essential to examine the effect of noise and signal in composite chaotic time signal. Recently, some studies have shown that filtering of noisy and stochastic signals from chaotic time series possibly affects the determination of nonlinear parameters (e.g. attractor dimension estimates and Lyapunov exponent). It has been noted that small scale noise shows

*For correspondence. (e-mail: postmast@csngri.ren.nic.in)